Structural and Multidisciplinary Optimization (2020) 61:1913–1928
https://doi.org/10.1007/s00158-019-02444-y

RESEARCH PAPER

A parameterized level set method combined with polygonal finite elements in topology optimization

Peng Wei[1] · Glaucio H. Paulino[2]

Received: 9 September 2018 / Revised: 22 September 2019 / Accepted: 23 October 2019 / Published online: 31 January 2020

Abstract
Level set-based topology optimization methods have received increased attention in the last decade due to the ease with which they can handle topology changes by splitting and merging boundaries. However, most implementations are limited to box-like design domains and cannot easily handle irregular domains that are common in practical engineering applications. In this paper, a modified level set model, which is parameterized and updated with radial basis functions (RBFs), is introduced to solve topology optimization problems in complex design domains. Because RBFs are not necessarily located in a structured manner, the parametrized level set method can be combined effortlessly with unstructured polygonal finite element meshes to easily handle complex design domains and also achieve the high accuracy characteristic of polygonal discretizations. Furthermore, the nucleation capability of the proposed approach along with an approximate reinitialization is shown to obtain more flexible topology changes of the optimal design, and smooth boundaries can be obtained without introducing smoothing scheme. Several numerical examples illustrate the effectiveness of the proposed model.

Keywords Topology optimization · Radial basis functions · Polygonal finite elements · Parameterized level set method

1 Introduction

Structural optimization methods have received increased attention during the last several decades because of their ability to achieve designs with increased mechanical performance and more efficient material use. Topology optimization in the continuum is one of the most prominent branches of the field. It has been used to obtain novel designs with flexible topologies for structures, materials, compliant mechanisms, among others. The continuum approach was first studied by Cheng and Olhoff (1981) when they investigated the optimal thickness distribution of elastic plates. Soon after, the homogenization method (Bendsoe and Kikuchi 1988) and its variations emerged as an important group of topology optimization models. Nowadays, the most popular method is the solid isotropic microstructure/material with penalization (SIMP) approach, which was proposed and developed by Bendsoe (1989) and Rozvany et al. (1992), and considers the density of each element to represent the distribution of material within the design. Sigmund's (2001) 99-line educational MATLAB code helped this approach spread widely at the beginning of this century.

Another popular density-based model is the evolutional structural optimization (ESO) method, which simply removes elements of low stress to approach an optimal design. The ESO method was first proposed by Xie and Steven (1993) and the bidirectional version of ESO (BESO) was developed a few years later (Querin et al. 1998; Huang and Xie 2010). This simple and easy-to-implement scheme as proven to be a powerful structural topology optimization method (Xia et al. 2018).

The level set method, which was first proposed by Osher and Sethian (1988), provides a more suitable way to deal with boundary-related optimization problems. It can easily deal

Responsible Editor: Seonho Cho

✉ Peng Wei
ctpwei@scut.edu.cn

✉ Glaucio H. Paulino
glaucio.paulino@ce.gatech.edu

[1] School of Civil Engineering and Transportation, State Key Laboratory of Subtropical Building Science, Guangdong Provincial Key Laboratory of Technique and Equipment for Macromolecular Advanced Manufacturing, South China University of Technology, 381 Wushan Rd., Guangzhou 510641, P. R. China

[2] School of Civil and Environmental Engineering, Georgia Institute of Technology, 790 Atlantic Drive, Atlanta, GA 30332, USA

with topology changes and has no difficulty handling the splitting and merging of boundaries. It has been implemented in topology optimization problems since 2000 (Sethian and Wiegmann 2000; Osher and Santosa 2001). Soon after, Wang et al. (2003) and Allaire et al. (2004) developed the optimization model based on the shape derivative and opened up a fruitful era for level set-based topology optimization methods. The level set-based topology optimization methods have been widely used in solving compliance minimization problems (Wang et al. 2003; Allaire et al. 2004), dynamic problems (Allaire and Jouve 2005; Yamada et al. 2010; Xia et al. 2011), acoustic–elastic coupled problems (Isakari et al. 2017), stress alleviation problems (Zhang et al. 2013; Picelli et al. 2018; Polajnar and Kosel 2017; Emmendoerfer et al. 2019), structure-material integrated design problems (Wang et al. 2016; Li et al. 2016), explicit structural representation problems (Guo et al. 2016; Zhou et al. 2016), feature control problems (Dapogny et al. 2017; Liu et al. 2017), and so on. Several review papers in this area summarize the recent developments (van Dijk et al. 2013; Gain and Paulino 2013; Sigmund and Maute 2013).

The conventional level set method is well developed in the field of computer graphics (CG). It consists of a set of numerical approaches such as updating the level set function on grid points by solving the Hamilton-Jacobi (H-J) equation, the velocity extension approach, and reinitialization scheme. In topology optimization, a set of variational level set methods have been developed. The piecewise constant level set method (Wei and Wang 2009), level set method with reaction-diffusion equation (Yamada et al. 2010), and the parameterized level set method are a few examples. In the parameterized level set model, the level set function is parameterized with a set of parameters, namely the expansion coefficients, and its evolution is realized by updating those parameters instead of solving the H-J equation as in the conventional model. The parameterized level set method was first introduced for topology optimization problems by Wang and Wang (2006) and Wang et al. (2007). In their study, radial basis functions (RBFs) were used to parameterize the discrete level set function to solve a more convenient ODE system instead of the H-J PDE in the conventional level set model. This method was implemented at almost the same time in image segmentation (Gelas et al. 2007) and later Xie and Mirmehdi (2011) implemented this approach in active contour and active surface models on segmenting textured color images. In general, the parameterized level set method has not been widely used in the field of topology optimization, perhaps because of its poor accuracy and efficiency (Gain and Paulino 2013). However, an improved version of the method that addressed these concerns was proposed together with an 88-line educational MATLAB code (Wei et al. 2018). This improved version was applied to topology optimization problems considering symmetry and pattern repetition constraints (Liu et al. 2018) and was shown to have good stability and applicability. The parameterized level set method can also be extended to an algebraic formulation in which the sensitivity with respect to the coefficients can be directly derived (Wang and Wang 2005, Wei and Wang 2006a, b, Luo et al. 2007, 2008, 2009). Recently, cardinal basis functions instead of RBFs revealed the clear physical meaning of the coefficients in this framework (Jiang et al. 2018).

In this paper, the improved parameterized level set method is adopted (Wei et al. 2018) and implemented effortlessly with unstructured polygonal meshes, enabling topology optimization on complex design domains that have practical applicability (Talischi et al. 2010, 2012a, b). This is in contrast to most of the literature on topology optimization problems using the conventional level set method, in which uniform grids in regular, box-like design domains dominate. In continuum topology optimization considering the SIMP method, polygonal finite elements (Sukumar and Tabarraei 2004) have been shown to naturally overcome the checkerboard problem observed with quadrilateral elements because they avoid single-point connections (Talischi et al. 2012b). Additionally, polygonal elements, which can be considered a natural extension of triangular and quadrilateral elements, have been shown to have better accuracy (Talischi et al. 2012a) than standard finite elements. Although some additional effort is typically needed to address the numerical difficulties in updating the level set function on an unstructured mesh (Barth and Sethian 1998), these problems are avoided in the parameterized level set method (Cecil et al. 2004).

An easy way to create polygonal FEM meshes in MATLAB platform was provided by Talischi et al. (2012a). Based on that, the topology optimization with the SIMP method (Talischi et al. 2012b) can be easily applied. In this study, the PolyMehser is also adopted, but the parametrized level set method with radial basis functions (Wei et al. 2018) is used instead of the SIMP model to perform the topology optimization. Only the problems in 2D are considered but it is not difficult to extend this model to higher dimensions (Cecil et al. 2004).

The remainder of this paper is organized as follows. In Section 2, a brief introduction of the parametrized level set method and its implementation in topology optimization is given. Then, several numerical schemes implemented in this framework with polygonal finite elements are studied. After that, some numerical examples are given to illustrate the properties and effectiveness of the proposed method. Finally, conclusions are provided.

2 Parameterized level set model with radial basis functions

In level set-based topology optimization, the boundary of design is represented in an implicit manner. For an n-dimensional design over a reference domain $D \subset R^n$, a one-dimensional higher scalar function, which is called level set function, $\Phi(x, t)$ is defined to represent the admissible shape $\Omega = \{x | \Phi(x) \geq 0, x \in D\}$ of the design with its implicit intersection with the zero level set. This representation scheme of a 2D design with level set function is illustrated in Fig. 1.

In Fig. 1, the design is obtained from the level set function as follows:

$$\begin{cases} \boldsymbol{x} \in D \backslash \Omega & \Phi(\boldsymbol{x}, t) < 0 \\ \boldsymbol{x} \in \partial\Omega \cap D & \Phi(\boldsymbol{x}, t) = 0 \\ \boldsymbol{x} \in \Omega \backslash \partial\Omega & \Phi(\boldsymbol{x}, t) > 0 \end{cases} \tag{1}$$

where $\partial\Omega$ represents the boundary of the design Ω.

The level set function $\Phi(\boldsymbol{x}, t)$ is updated to trace the moving boundary by introducing the pseudo-time t and then solving the following Hamilton-Jacobi equation:

$$\frac{\partial \Phi(\boldsymbol{x}, t)}{\partial t} - |\nabla \Phi(\boldsymbol{x}, t)| V_n(\boldsymbol{x}, t) = 0 \tag{2}$$

where V_n is the component of the velocity of the free boundary in the direction of the outer normal direction $\vec{n}$:

$$V_n = \vec{V} \cdot \left(-\frac{\nabla \Phi}{|\nabla \Phi|} \right) \tag{3}$$

where $\vec{V}$ denotes the velocity vector of the free boundary.

In the conventional level set model, once V_n is determined using shape derivatives, the H-J equation is solved iteratively to evolve the free boundary in an Eulerian manner to achieve the optimal design. The solution of H-J equation and the reinitialization scheme are generally performed on structured meshes, while the finite element analysis for the calculation of the velocity field V_n to update the H-J equation needs to be performed on an unstructured mesh in order to handle complex design shapes and boundary conditions. In this case, the finite element mesh is not consistent with the mesh used in the level set model and excessive effort is needed to map the velocity field back and forth between the two sets of meshes. This strategy is not practical for integration into mature CAE systems for realistic engineering applications. Therefore, if the level set method is to be accepted by industry, both the solution of the H-J equation and the finite element analysis for calculation of V_n must be performed on the same mesh. To implement the conventional level set method on an unstructured mesh is difficult (Barth and Sethian 1998). Thus, in the present study, the parameterized level set method, which is shown to be insensitive to the mesh type, is used to explore the possible application of the level set method in industry applications.

In the parameterized level set model, the level set surface is represented with a set of expansion coefficients for radial basis function interpolation. Thus, the evolution of the level set surface is updated in a parameter space instead of on a discrete grid as in the conventional level set model and the dependence on a structured grid to solve the H-J equation can be totally eliminated. With this approach, the level set function can be combined with any type of finite elements and enable the solution of complex problems on irregular design domains. Because the boundary representation is still implicit, the advantages of the conventional level set method, i.e., flexible topology change and smoothness of the boundary, are maintained. Additionally, the reinitialization scheme can be replaced by an easy-to-implement approach, which does not prevent nucleation capacity inside the design domain.

Radial basis functions are a set of functions that are widely used in numerical interpolation. Here we implement this technology to parameterize the level set function to obtain some numerical benefits.

A radial basis function $g : R^d \rightarrow R$ can be expressed as follows:

$$g_i(\boldsymbol{x}) = g\left\| \boldsymbol{x} - \bar{\boldsymbol{x}}_i \right\| \tag{4}$$

where $\bar{\boldsymbol{x}}_i$ is the coordinate of the knot where the radial basis function is centrally located and $\|\cdot\|$ is the Euclidean norm on R^d. Thus, the level set function at the jth point $\boldsymbol{x}_j$ can be represented by a linear combination of a set of N radial basis functions as follows:

$$\Phi(\boldsymbol{x}_j, t) = \sum_{i=1}^{N} g_i(\boldsymbol{x}_j) \alpha_i(t) \tag{5}$$

or in vector form:

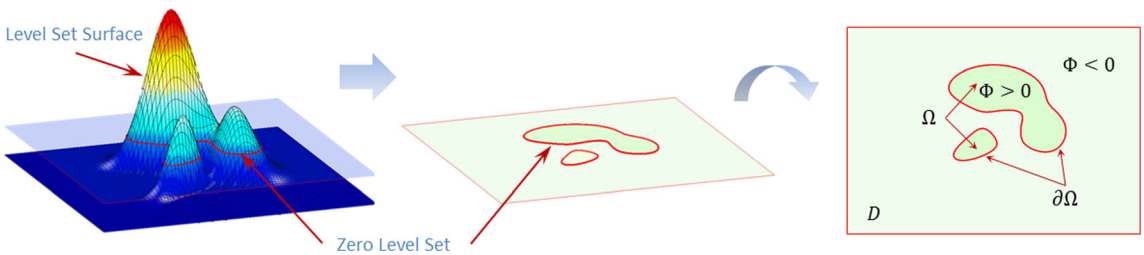

Fig. 1 A 2D design and the level set function used to represent it

$$\Phi(\boldsymbol{x}_j,t)=\boldsymbol{G}(\boldsymbol{x}_j)^T\alpha(t) \tag{6}$$

where

$$\boldsymbol{\alpha}=\{\alpha_1,\alpha_2,\cdots,\alpha_N\}^{\mathbf{T}} \tag{7}$$

$$\boldsymbol{G}(\boldsymbol{x}_j)=\left[g_1(\boldsymbol{x}_j),g_2(\boldsymbol{x}_j),\cdots,g_N(\boldsymbol{x}_j)\right]^{\mathbf{T}} \tag{8}$$

where α_i is the expansion coefficient of the ith radial basis function. Equation (6) can also be written in a matrix form if x denotes M points $\boldsymbol{x}_1,\boldsymbol{x}_2,\cdots,\boldsymbol{x}_{\mathbf{M}}$. The level set function can be represented as:

$$\boldsymbol{\Phi}(\mathbf{x},t)=\boldsymbol{A}(\mathbf{x})\cdot\boldsymbol{\alpha}(t) \tag{9}$$

where

$$\mathbf{x}=\{\boldsymbol{x}_1,\boldsymbol{x}_2,\cdots,\boldsymbol{x}_M\}^{\mathbf{T}} \tag{10}$$

$$\begin{aligned}\boldsymbol{A}(\mathbf{x})&=[G(\boldsymbol{x}_1),G(\boldsymbol{x}_2),\cdots,G(\boldsymbol{x}_N)]^T\\&=\begin{bmatrix}g_1(\boldsymbol{x}_1)&\cdots&g_N(\boldsymbol{x}_1)\\\vdots&\ddots&\vdots\\g_1(\boldsymbol{x}_M)&\cdots&g_N(\boldsymbol{x}_M)\end{bmatrix}\end{aligned} \tag{11}$$

$$\boldsymbol{\Phi}(\mathbf{x},t)=\{\Phi(\boldsymbol{x}_1,t),\Phi(\boldsymbol{x}_2,t),\cdots,\Phi(\boldsymbol{x}_M,t)\}^T \tag{12}$$

If the values of the level set function on the knots are known as $\Phi(\overline{\mathbf{x}})$, where $\overline{\mathbf{x}}$ denotes the coordinates of the knots, the expansion coefficients can be obtained by solving the following equation using a collocation approach in which $N=M$:

$$\boldsymbol{\alpha}(t)=\boldsymbol{A}\left(\overline{\mathbf{x}}\right)^{-1}\boldsymbol{\Phi}\left(\overline{\mathbf{x}},t\right) \tag{13}$$

This approach is usually used in the beginning stage to determine the initial value of $\boldsymbol{\alpha}$ after the initial level set function was given or when the discrete level set function is reconstructed and then to recalculate the value of $\boldsymbol{\alpha}$. In this method, the expansion coefficients $\boldsymbol{\alpha}$ are the parameterized design variables instead of the values of the level set function on all the grid points as in the conventional level set method. The optimization process can be considered as the approach to update $\boldsymbol{\alpha}$ according to the related information with the following equation:

$$\boldsymbol{\alpha}^{k+1}=\boldsymbol{\alpha}^k+\tau\Delta\boldsymbol{\alpha} \tag{14}$$

where $\boldsymbol{\alpha}^k$ indicates the $\boldsymbol{\alpha}$ value in the kth iteration, τ is the step size and $\Delta\boldsymbol{\alpha}$ is the increment in each step, which can be determined by the sensitivity analysis introduced later. A graphical representation of a 1D case of the parametrization scheme with three basis functions is given in Fig. 2. The basis function g_i is located in $\boldsymbol{x}_i$ and the level set function can be represented by the linear combination of the three basis functions.

Many different kinds of radial basis functions can be implemented in this model, such as Gaussians, multiquadrics (MQ), inverse multiquadrics (IMQ), which are all globally supported radial basis functions (GSRBFs), and Wendland's compactly supported RBFs (CSRBFs) (Wendland 1995). In this model, numerical tests did not show much difference based on the choice of RBF, but it should be noted that for multiquadrics, a side constraint is needed in Eq. (5) (Wang et al. 2007).

With the radial basis function interpolation, substituting Eq. (5) into Eq. (2), one can obtain that

$$\boldsymbol{A}\frac{d\boldsymbol{\alpha}}{\mathrm{d}t}-\overline{\boldsymbol{V}}_n=0 \tag{15}$$

where

$$\overline{\boldsymbol{V}}_n=\left\{\begin{array}{l}\left|\nabla\boldsymbol{G}(\boldsymbol{x}_1)^T\cdot\boldsymbol{\alpha}\right|\boldsymbol{V}_n(\boldsymbol{x}_1)\\\left|\nabla\boldsymbol{G}(\boldsymbol{x}_2)^T\cdot\boldsymbol{\alpha}\right|\boldsymbol{V}_n(\boldsymbol{x}_2)\\\quad\vdots\\\left|\nabla\boldsymbol{G}(\boldsymbol{x}_M)^T\cdot\boldsymbol{\alpha}\right|\boldsymbol{V}_n(\boldsymbol{x}_M)\end{array}\right\} \tag{16}$$

Considering the expansion coefficients $\boldsymbol{\alpha}$ changing according to pseudo-time t, implementation first-order time discrete differential algorithm is

$$\frac{d\boldsymbol{\alpha}}{\mathrm{d}t}\approx\frac{\boldsymbol{\alpha}^{k+1}-\boldsymbol{\alpha}^k}{\Delta t} \tag{17}$$

Thus, Eq. (15) can be written as:

$$\boldsymbol{\alpha}^{k+1}=\boldsymbol{\alpha}^k+\Delta t\cdot\boldsymbol{A}^{-1}\overline{\boldsymbol{V}}_n^k \tag{18}$$

where Δt is a time step in first-order time discrete updating scheme. $\overline{\boldsymbol{V}}_n^k$ is the normal velocity field $\overline{\boldsymbol{V}}_n$ obtained in the kth step by sensitivity analysis. $\boldsymbol{A}^{-1}$ and $\nabla\boldsymbol{G}^T$ are only related to the locations of the knots and the type of the radial basis function. If the locations of the knots are all fixed during the optimization process, A^{-1} and ∇G^T are also determined and only need to be calculated once during pre-processing and stored.

The Eq. (18) is derived from the H-J equation (Eq. 2) and it has been applied many times in the literature. However, in practical implementation, the direct use of Eq. (18) in this framework may cause numerical instabilities. Thus, a normalization scheme in which the magnitude of the gradient is used as an inverse weight is used (Xie and Mirmehdi 2011; Wei et al. 2018):

$$\boldsymbol{\alpha}^{k+1}=\boldsymbol{\alpha}^k+\Delta t\cdot\boldsymbol{A}^{-1}\boldsymbol{V}_n^k \tag{19}$$

where

$$\boldsymbol{V}_n^k=\left\{\begin{array}{cccc}V_n^k(x_1)&V_n^k(x_2)&\ldots&V_n^k(x_M)\end{array}\right\}^T \tag{20}$$

and the superscript k indicates the kth step. Obviously, this update equation is simpler than Eq. (18) and the associated computational cost is also improved. In addition, the evolution process becomes more stable and no filter is needed to keep the boundary smooth.

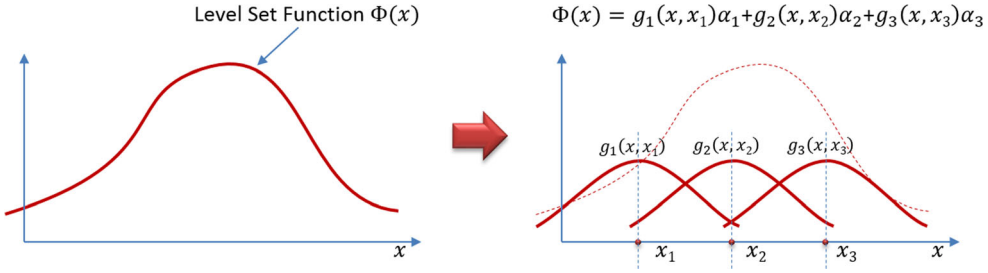

Fig. 2 The parameterization scheme of a level set function in the 1D case

Another important property should be noted in Eq. (19): the level set function is updated with the expansion coefficients instead of the discrete spatial difference as in the conventional level set method. By parameterizing with radial basis functions, the gradients are now considered in parameter space and the evolution equation is transformed into an ODE of α instead of a PDE. This makes the solution procedure easier compared with the conventional level set method. Furthermore, because of the radial basis interpolation, there are no restrictions on the mesh. In the present work, the unstructured polygonal finite element meshes are used to allow for more flexible geometry of the design domain.

3 Structural optimization with RBF-based parameterized level set method

Several variations of the level set method have been used for structural optimization starting at the beginning of this century. The RBF-based parameterized level set method takes advantage of the parameterization with which the PDE is transformed into an ODE in tracing the front surface during the evolution of the structure.

The structural topology optimization problem with the level set model can be represented as follows:

$$\begin{aligned} &\underset{\Phi}{\text{Minimize}} && \mathrm{J}(\mathbf{u},\Phi) = \int_D \mathrm{f}(\mathbf{u})\mathrm{H}(\Phi)\mathrm{d}\Omega \\ &s.t. && a(\mathbf{u},\mathbf{v},\Phi) = l(\mathbf{v},\Phi),\ \mathbf{u}|_{\Gamma_D} = \mathbf{u}_0, \quad \forall \mathbf{v} \in \mathrm{U} \\ & && \mathrm{V}(\Phi) \le \mathrm{V}_0 \\ & && a(\mathbf{u},\mathbf{v},\Phi) = \int_D \boldsymbol{\varepsilon}^{\mathrm{T}}(\mathbf{u})\mathbf{C}\boldsymbol{\varepsilon}(\mathbf{v})\mathrm{H}(\Phi)\mathrm{d}\Omega \\ & && l(\mathbf{v},\Phi) = \int_D \mathbf{p}\mathbf{v}\mathrm{d}\Omega + \int_{\Gamma_\mathrm{N}} \boldsymbol{\tau}\mathbf{v}\mathrm{d}\Gamma \end{aligned} \tag{21}$$

where J is the objective function, which represents the compliance of the design in this study, f is the integration function in the objective, $\mathbf{u}$ is the displacement vector, H is the Heaviside function, a is the bilinear form of the energy, l is the linear form of the load, $\mathbf{v}$ is denotes the virtual displacement field belonging to the kinematically admissible displacement fields U, $\mathbf{u}_0$ is the prescribed displacement on the admissible Dirichlet boundary Γ_D, V is the total volume of the design, V_0 is the upper bound of the volume, $\boldsymbol{\varepsilon}$ is the strain field, $\mathbf{C}$ is the elasticity tensor, $\mathbf{p}$ are the body forces, and $\boldsymbol{\tau}$ are the boundary tractions applied on Neumann boundary Γ_N. The elastic equilibrium equation is shown in the variational weak form.

The sensitivity analysis of this problem can be solved based on the shape derivative theory to obtain the update scheme of the level set function to minimize the objection under the given constraints. The Lagrangian of the optimization problem can be written as:

$$\begin{aligned} \mathrm{L}(\mathbf{u},\mathbf{v},\Phi) = J(\mathbf{u},\Phi) + \lambda(\mathrm{V}(\Phi)-\mathrm{V}_0) - l(\mathbf{v},\Phi) \\ + a(\mathbf{u},\mathbf{v},\Phi) \end{aligned} \tag{22}$$

where λ is the Lagrange multiplier for the inequality volume constraint to restrict material consumption. The shape derivative of the problem can be reduced by involving a pseudo-time t, which represents the iteration step for the boundary evolution. The derivative of the Lagrangian with respect to t can be written as:

$$\frac{d\mathrm{L}(\mathbf{u},\mathbf{v},\Phi)}{dt} = \int_D \beta(\mathbf{u},\mathbf{v},\Phi)\delta(\Phi)|\nabla\Phi|V_n\mathrm{d}\Omega \tag{23}$$

where $\delta(\Phi)$ is the derivative of the Heaviside function and β can be derived as (Wang et al. 2003; Allaire et al. 2004):

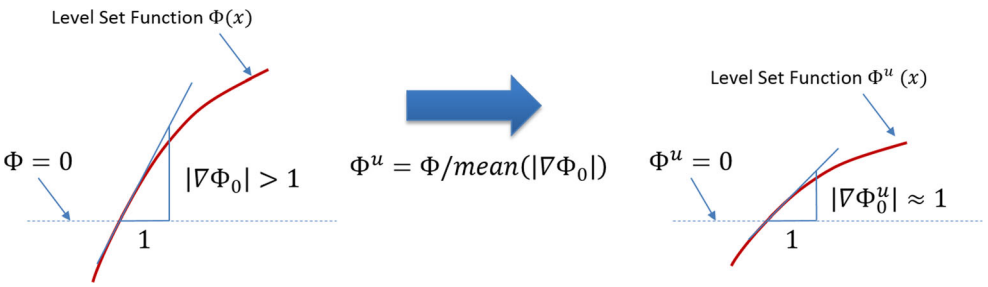

Fig. 3 The updating scheme of the approximate reinitialization process

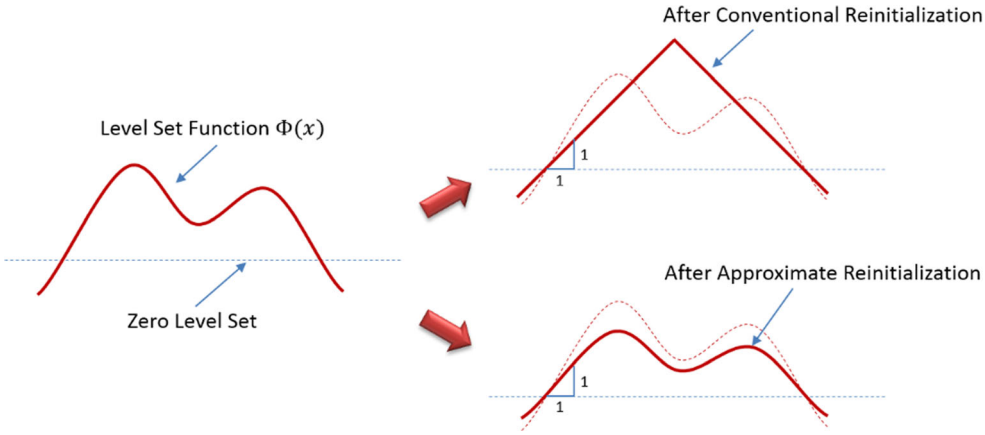

Fig. 4 The comparison between the conventional and the approximate reinitialization schemes

$$\beta(\mathbf{u},\mathbf{v},\Phi) = \mathrm{f}(\mathbf{u}) - \boldsymbol{\varepsilon}^T(\mathbf{u})\mathbf{C}\boldsymbol{\varepsilon}(v) + (\mathrm{pu} + \nabla(\tau\mathrm{v})\cdot n + \kappa(\tau\mathrm{v})) + \lambda \tag{24}$$

where $\kappa = \nabla \cdot (-\nabla \Phi/|\nabla\Phi|)$ is the mean curvature.

One key point in the level set-based method is the calculation of the velocity V_n in Eq. (23) based on the sensitivity analysis, which has been provided by Wang et al. (2003) and Allaire et al. (2004) in detail. The velocity V_n is given as $-\beta$ at each iteration step to keep the derivative of the Lagrangian negative to approach the optimum iteratively. The Lagrange multiplier λ can be obtained with the augmented Lagrange method (Wei and Wang 2006b; Wei et al. 2018) or the bisection method (Sigmund 2001).

For compliance minimization, which is considered in the present work

$$\mathrm{f}(\mathbf{u}) = \boldsymbol{\varepsilon}^T(\mathbf{u})\mathbf{C}\boldsymbol{\varepsilon}(\mathbf{u}) \tag{25}$$

and the optimization problem can be shown to be self-adjoint in which $\mathbf{v} = 2\mathbf{u}$. If body forces and tractions are not considered, the normal velocity can be simplified as:

$$V_n = \boldsymbol{\varepsilon}^T(\mathbf{u})\mathbf{C}\boldsymbol{\varepsilon}(\mathbf{u}) - \lambda \tag{26}$$

which indicates that the prominent factors in optimization are the strain energy density along the boundary and the Lagrange multiplier. For more details of the derivation, readers can refer to the references (Wang et al. 2003, Allaire et al. 2004).

The velocity field can be obtained with the polygonal finite element analysis according to Eq. (26) and substituted into Eq. (18) to update the expansion coefficients α and then, the level set function in each iteration step to evolve the design and pursue the optimum.

4 Implementation schemes

Some numerical schemes need to be included in the level set-based topology optimization framework. For example, in the conventional level set model, the level set function may become flatter or steeper after several iterations, causing instabilities during the boundary evolutions. Thus, a reinitialization

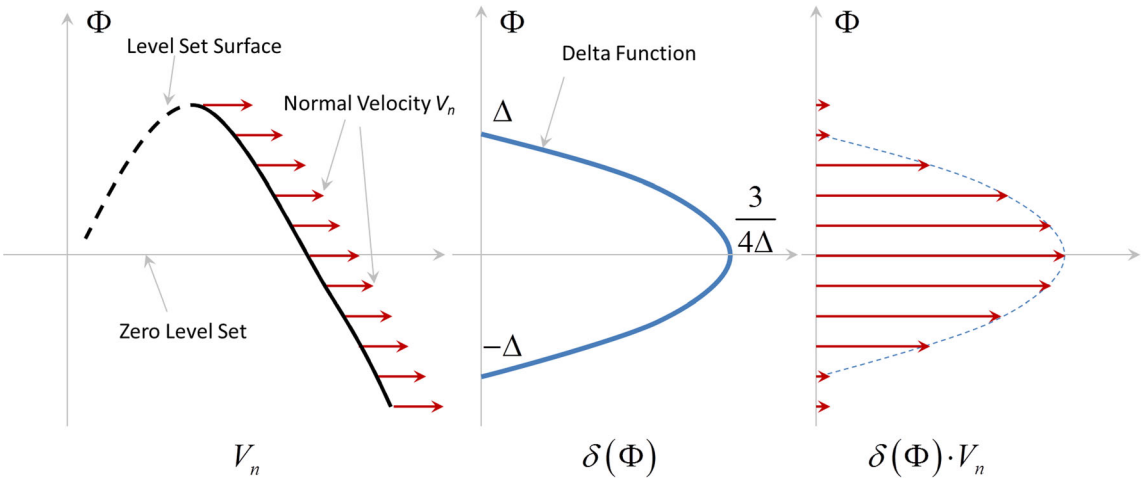

Fig. 5 The effect of the $\delta(\Phi)$ function multiplying the normal velocity

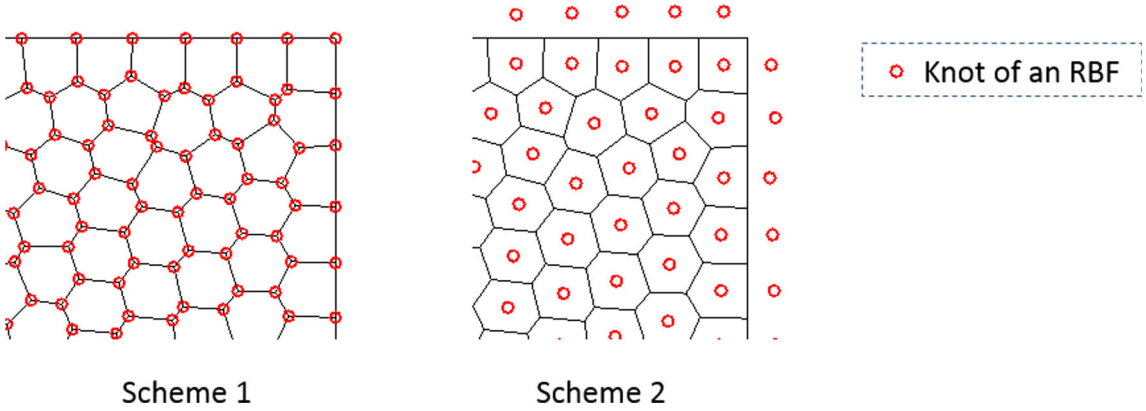

Fig. 6 Two schemes to locate the knots in the RBF interpolation scheme

scheme, e.g., a PDE-driven method (Peng et al. 1999) or a fast marching method (Sethian 1999), is needed to keep the level set function a signed distance surface with $|\nabla\Phi(\boldsymbol{x}, t)| = 1$ of which the angle is 45 degrees to the zero level set. This approach makes the iteration process more accurate and stable. However, these conventional reinitialization schemes cannot be implemented directly in a parameterized space. Instead, the coefficients have to be mapped to the discrete space and mapped back after reinitialization. Furthermore, reinitialization on an unstructured mesh complicates the numerical implementation and increases the computational cost in the parametrized level set framework. Therefore, in this model, an approximate reinitialization process is applied to improve the slope of the level set function with mush less complexity. The update level set function value $\boldsymbol{\Phi}^u$ is obtained using Eq. (27).

$$\boldsymbol{\Phi}^u = \frac{\boldsymbol{\Phi}(\mathbf{x})}{mean(|\nabla\boldsymbol{\Phi}_0|)} \tag{27}$$

where $\boldsymbol{\Phi}(x)$ is the level set surface and $\boldsymbol{\Phi}_0$ are the values of the level set function around the zero level set and mean(f) denotes the mean value of the function f. Because of the linear relation with $\boldsymbol{\Phi}(\mathbf{x})$ and α according to Eq. (9), Eq. (27) can be rewritten as:

$$\boldsymbol{\alpha}^u = \frac{\boldsymbol{\alpha}}{\text{mean}(|\nabla\boldsymbol{\Phi}_0|)} \tag{28}$$

Figure 3 illustrates the approximate reinitialization scheme. This approach can be easily applied in the whole design domain to keep the slope of the level set function around the boundary almost constant. Compared with conventional

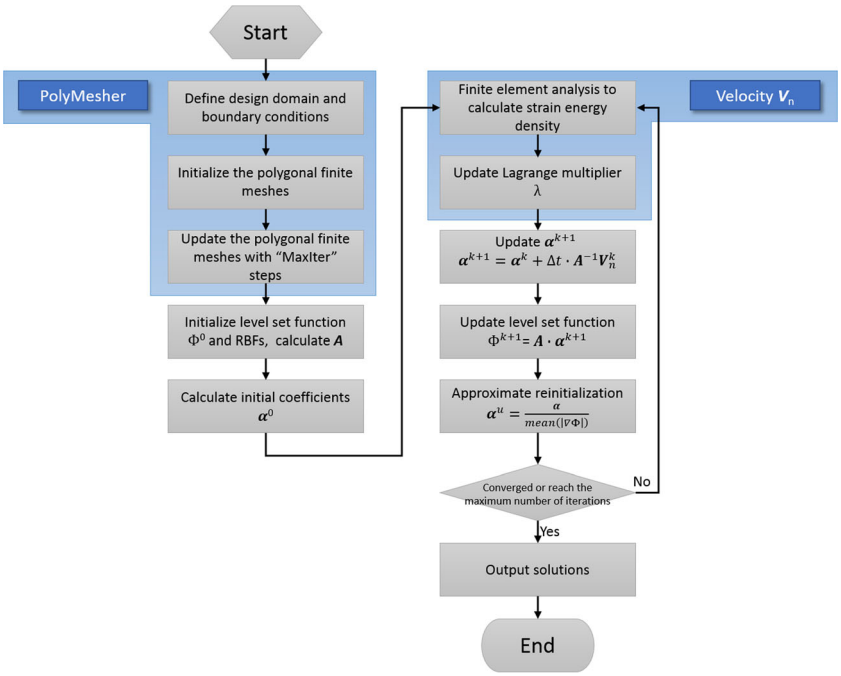

Fig. 7 The flowchart of the proposed method

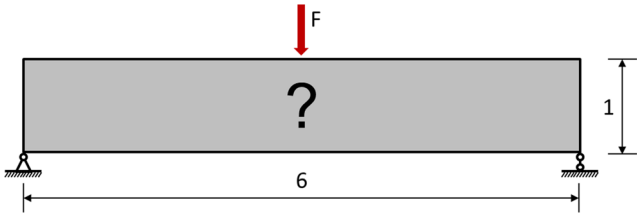

Fig. 8 The MBB beam problem

reinitialization schemes, this approach has no difficulty in numerical implementation even on unstructured meshes, and it does not change the boundary as conventional reinitialization schemes do. Furthermore, because this scheme only changes the relative value of the level set function and does not remove concave features (Fig. 4), it does not prevent nucleation. This reinitialization scheme was introduced by Wei et al. (2018) for structured meshes and extended to unstructured meshes without any additional difficulties.

Since in this RBF-based level set method, the reinitialization scheme is not necessarily involved, the values of level set function may grow unboundedly and make the surface extremely steep (Gain and Paulino 2013). This is not a fatal issue of this method, but still may cause instabilities and convergence issues. Therefore, in the present work, an approximate function $\delta(\Phi)$ is included in the update scheme to avoid unbounded growth of the level set surface as introduced in Wei et al. (2018). The $\delta(\Phi)$ function is used as follows (Wang et al. 2003):

$$\delta(\Phi)=\begin{cases}0, & \Phi>\Delta\\ \dfrac{3}{4\Delta}\left(1-\dfrac{\Phi^2}{\Delta^2}\right), & -\Delta<\Phi<\Delta\\ 0, & \Phi<-\Delta\end{cases} \tag{29}$$

Thus, the level set surface updating equation is modified to:

$$\frac{d\Phi}{dt}-\delta(\Phi)V_n=0 \tag{30}$$

In Eq. (29), the parameter Δ is used to control the magnitude of the highest and the lowest part of the level set function.

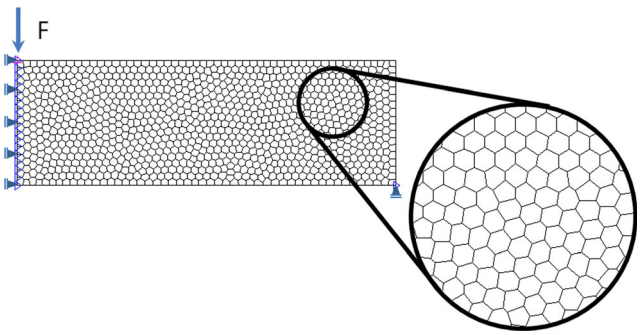

Fig. 9 The polygonal mesh for the MBB beam problem

As long as it is large enough, the absolute value of Δ need not be an exact value. The effect of the $\delta(\Phi)$ function is illustrated in Fig. 5. Notice that when Φ equals to 0, i.e., zero level set, $\delta(\Phi)$ equals to $0.75/\Delta$; thus, according to Eq. (30), the effect of the value of $\delta(\Phi)$ is equivalent to magnifying the normal velocity by $0.75/\Delta$ times on the zero level set. Thus, the normal velocity V_n should be divided by $0.75/\Delta$ when implementing Eq. (30) to keep the normal velocity on the zero level set unchanged. The normal velocity on the level set surface above Δ and below $-\Delta$ will vanish as a result of multiplying the $\delta(\Phi)$ function to prevent Φ from approaching infinity.

Because the level set update scheme is transformed into a parametric space spanned by the RBF interpolations, there is no rigorous restriction on the locations of the knots as long as the whole design domain is covered by the RBFs. Two schemes for the locations of the knots can be implemented in this framework as illustrated in Fig. 6. The red circles are the knots of RBF interpolation in both of the two schemes. In the first scheme, the knots are located at the nodes of the finite elements and the number of the RBFs is equal to the number of the nodes. This scheme is straightforward and easy to implement. However, in a polygonal mesh, the number of nodes is typically much larger than the number of the elements. Thus, the number of the RBFs is also large, which may affect the efficiency of updating the level set function and cause a large memory requirement. The second scheme is to locate the knots on the center of each element as illustrated in the right figure in Fig. 6. In this scheme, the number of knots is much less than in the first one. The number of knots is roughly equal to the number of elements, but some extra knots, located outside the boundary of the design domain, are needed to keep the values of the level set function on the boundary reasonable. There are no strict rules for the locations of these points, but they should be on or outside the boundary, not too far away from the boundary, and the level set values at these points should be restricted to zero. If the program of PolyMesher (Talischi et al. 2012a) is used to generate the polygonal finite element mesh, these points can be represented by the reflection points which are obtained in line 16 of the main program: `R_P = PolyMshr_Rflct(P, NElem, Domain, Alpha);`

Generally, with the second scheme, the total number of the knots may be 15–20% more than the number of elements for a rectangle design domain. But in the first scheme, the number of knots may be near twice as many as the number of elements. Thus, the second scheme is recommended here because of the higher efficiency and less memory requirement.

With this scheme, the proposed method can be implemented in different kinds of finite element meshes, e.g., quadrilateral, triangular, and polygonal, without extra processing of the level set method. The scheme also does not restrict on the

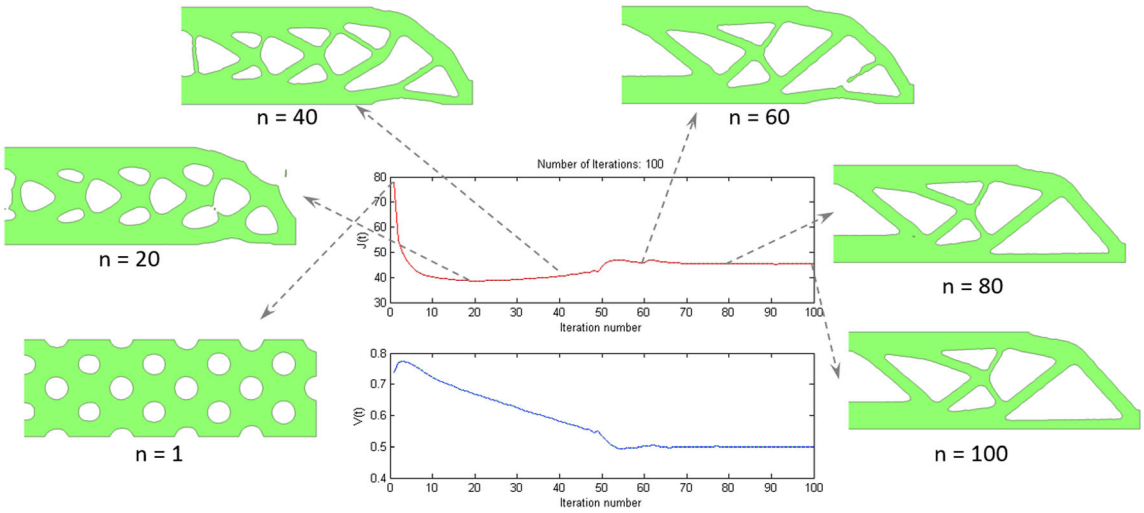

Fig. 10 Iteration history of the optimization process

shape of the design domain, which allows for more general and practical optimization problems.

The flowchart of the proposed method is illustrated in Fig. 7.

5 Numerical examples

In this section, several numerical examples are studied to verify the effectiveness and illustrate the properties of the proposed approach. The PolyMehser (Talischi et al. 2012a) is adopted to combine with the parametrized level set method with radial basis functions to perform the topology optimization. In all examples, the Ersatz method is applied such that Young's modulus $E = 1$ for solid elements and $E = 10^{-3}$ for void elements. Poisson's ratio is 0.3.

5.1 An MBB beam

The first example is an MBB beam shown in Fig. 8.

The size of the MBB Beam is 6-by-1. The downward force applied in the middle is F = 1. For simplicity, only the right half of the beam is solved.

Figure 9 shows the polygonal mesh used to solve the MBB beam problem. This mesh is obtained after 2000 iterations of PolyMesher (Talischi et al. 2012a). The design domain is discretized into 1000 elements with 2002 nodes. The knots are located at the nodes of the mesh, i.e., the total number of the knots is 2002. The multiquadric (MQ) splines given in Eq. (32) is used with $c = 10^{-3}$. The total number of iterative steps is 100. The iteration histories of the topology change, objective function, and volume fraction are illustrated in Fig. 10. The volume fraction is set as 0.5 and controlled with the augmented Lagrange method (Wei et al. 2018). The final objective function is 45.31 after 100 iterations.

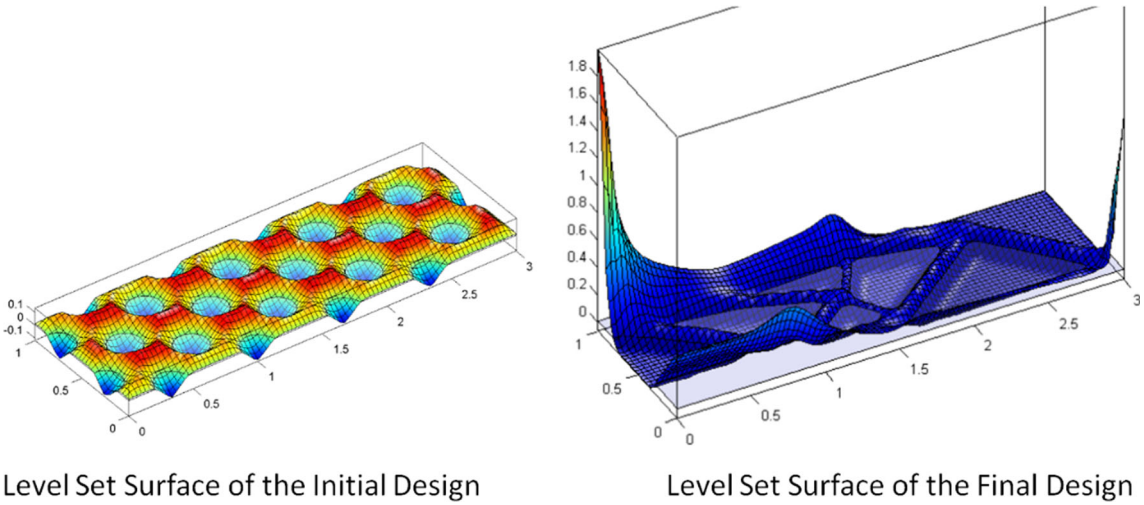

Fig. 11 The level set surfaces of the initial and the final design

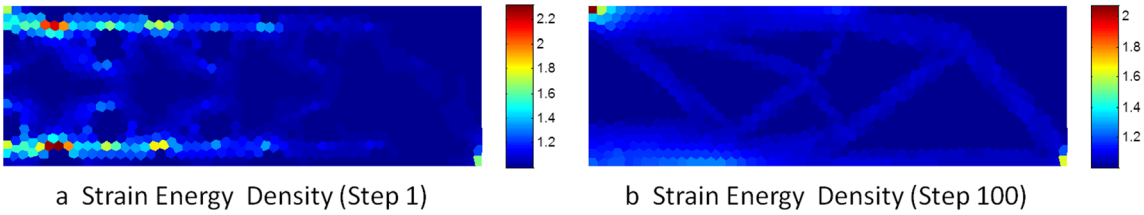

Fig. 12 The strain energy density distribution comparison

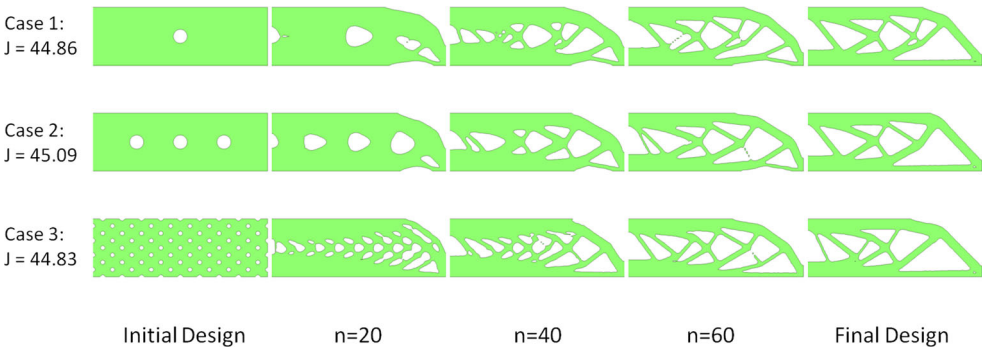

Fig. 13 Three optimization cases with different initial guesses

The level set surface of the initial and the final design are shown in Fig. 11. The level set function is initialized as a signed distance function as given in Eq. (31) which is used in most of the traditional applications.

$$\Phi^D(\boldsymbol{x}) = Sign(\Phi(\boldsymbol{x}))\cdot Dist(\boldsymbol{x}) \tag{31}$$

where $Sign(\cdot)$ is the sign of the function and $Dist(\cdot)$ is the distance of point to the boundary.

The final design is apparently not a signed distance function because the approximated reinitialization scheme is applied instead of the conventional one. But, it can be observed that in the areas around the boundaries, the level set surface is approximately a signed distance function because the surface update scheme is applied as given in Eq. (27).

The strain energy density distributions of the designs of the 1st step and the last step are illustrated in Fig. 12. It can be found around the boundary the strain energies are almost equal everywhere which indicates the optimal design.

5.1.1 Effect of the initial design

The initial design-dependent problem is always an important issue for level set-based topology optimization. With different initial guesses, different optimal designs may be obtained. One important reason in the conventional level set method is the lack of nucleation capability. In this study, by replacing Eq. (2) with Eq. (30), the conservational law is not held anymore, and by applying the natural velocity extension (Wang and Wang 2006), which means the velocity V_n is calculated in the whole design domain instead of around the boundary, and according to Fig. 4, the approximate reinitialization scheme does not prevent the nucleation, thus the level set function can create new holes automatically during the optimization iterative process. Figure 13 shows several optimal results with different initial designs. The total number of iterations is 300 in all cases and the finial objective function values are provided in the left column.

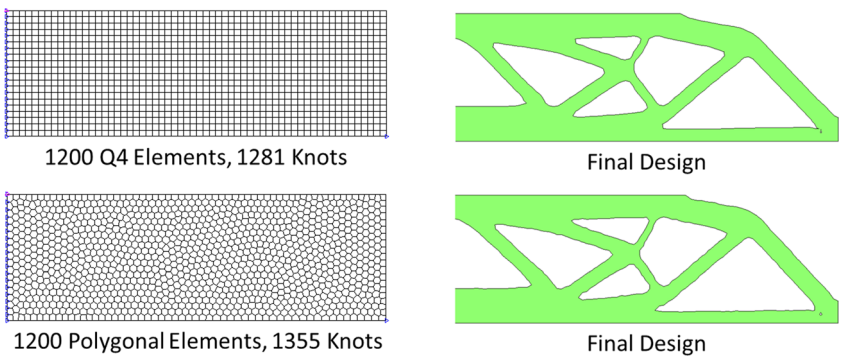

Fig. 14 The effect of different mesh types

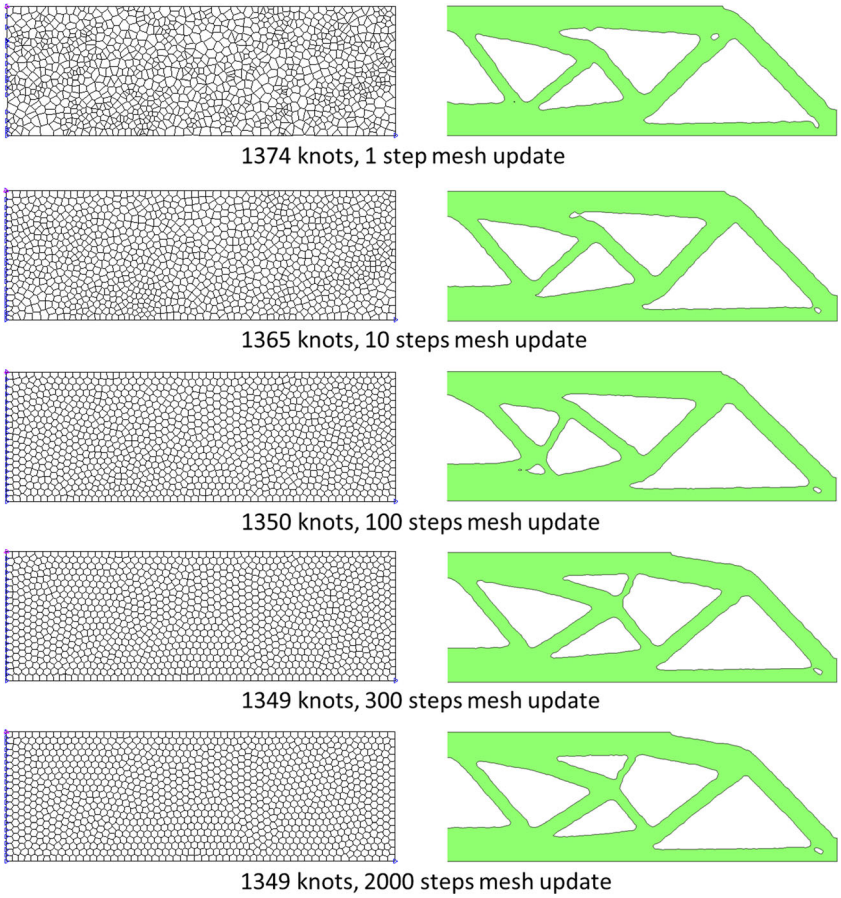

Fig. 15 The effect of different mesh quality

According to Fig. 13, the proposed method can create interior holes to change the topology. The final designs are different but they have similar topologies and objective function values. Besides the initial design, other factors such as the parameters in volume control during the optimization process also affect the final topology. Therefore, it is hard to totally eliminate the dependence on the initial design.

Note that there is no boundary smoothing scheme (e.g., filter or perimeter control) implemented in this study, and the proposed method can still provide relatively smooth boundaries. However, small holes do occur in the low-stress areas in the results in Fig. 13. The small holes can be removed by applying the smoothing schemes.

5.1.2 Effect of mesh type and quality

Figure 14 shows the final topology of the problem with two different meshes. The first design is obtained with Q4 elements and the second one with polygonal finite elements.

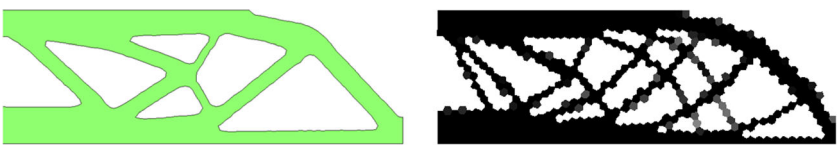

Fig. 16 The optimal design comparison between the proposed method (left) and the SIMP method (right)

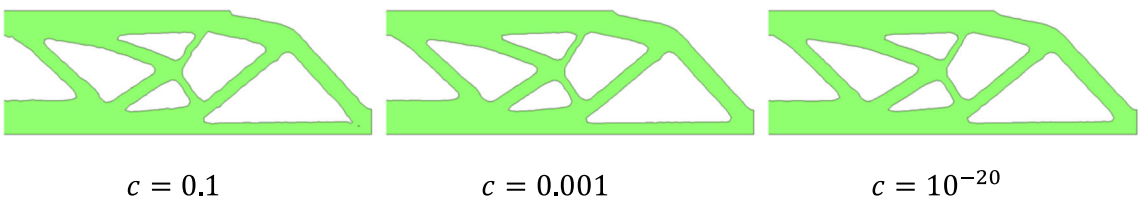

Fig. 17 The optimal results of MBB beam with MQ RBF in different values of c

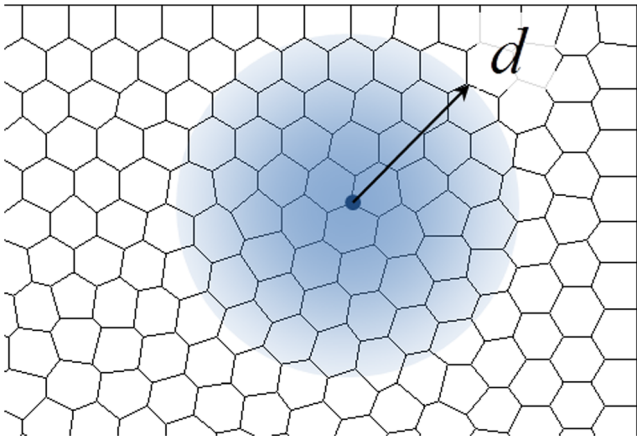

Fig. 18 The actual support radius of a CSRBF

The similarity in the topology of the two designs illustrates that the proposed method is insensitive to the meshes.

However, the quality of the finite element mesh may affect the optimal design. Figure 15 illustrates the optimal designs with different mesh qualities. The polygonal finite element meshes are obtained with the open source MATLAB code "PolyMesher" (Talischi et al. 2012a). The larger the "MaxIter" parameter in PolyMesher, the better the quality of the mesh. Generally, this parameter is larger than 500 to make sure the quality of the mesh is good enough. In this test case, all the meshes are obtained from the same set of initial mesh seeds, but with different numbers of updating steps. During the updating, some nodes may merge together; thus, the total number of nodes reduces as the number of updating steps increases. All the other parameters in the optimization are the same and the total number of optimization iterations is 500. It can be seen that the topologies of the final designs converge when the mesh update number increasing. Bad quality of the finite elements induces more instability during the optimization process and slow convergence in the same situation (same set parameters). So the mesh updating step number is suggested to be more than 300 according to this comparison.

5.1.3 Comparing with SIMP method

A comparison of the proposed level set approach and the SIMP method is shown in Fig. 16. The results illustrate the SIMP method provides a structure with more details and lower objective (mean compliance). One understandable reason is that it is more difficult to represent tiny details with the implicit boundary representation approach of the level set method. Another unproven reason is that the RBFs may produce a smoothing effect to some extent. This can also explain why the proposed method has no need to implement additional regularization schemes, such as a filter or perimeter control. Compared with the level set-based approach, the density-based method always shows zigzag boundary which is a traditional issue in topology optimization and generally a further post-processing approach is needed to smooth the surface of the design.

5.1.4 Parameter studies in RBFs

In this section, some important parameters of two types of RBFs, multiquadric (MQ) RBF, and Wendland's C2 CSRBF (Wendland 1995) are studied. MQ can be written as follows:

$$g(\boldsymbol{x}) = \sqrt{\left\|\boldsymbol{x}-\bar{\boldsymbol{x}}_i\right\|^2 + c^2} \tag{32}$$

where $c \geq 0$ is the parameter of MQ RBF. Figure 17 illustrates the results of the MBB beam with different values of c, and it can be seen that the final results are insensitive to this parameter so the value of c is easy to set. Then, the value of c will not affect the solutions as long as it is given a reasonable value which will not induce large numerical errors, i.e., a value less than 0.1.

Another popular set of RBFs are Wendland's CSRBFs which have limited support radius, the one with C2 continuity is C2 CSRBF which can be written as:

$$g(\boldsymbol{x}) = max\left\{0, (1-r)^4\right\}\cdot(4r+1) \tag{33}$$

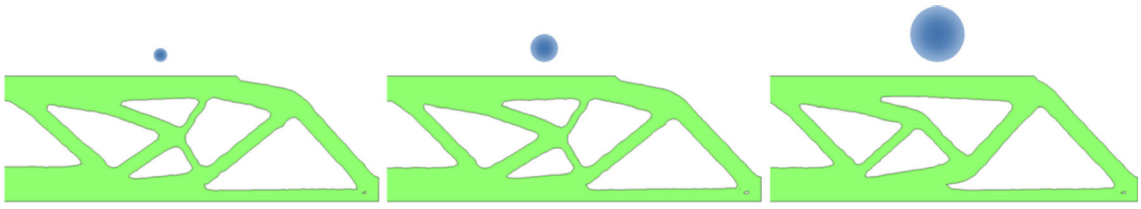

$d = 0.1095$ $d = 0.2191$ $d = 0.4382$

Fig. 19 The optimal results of MBB beam with C2 CSRBF with different support radii (corresponding to $n = 2, 4, 8$ respectively) and the blue circles show the actual support ranges

a The problem definition. b The result of the SIMP method. c The result of the proposed method.

Fig. 20 The optimal results of the hook example of the SIMP method and the parameterized level set method (**a**–**c**).

where

$$r = \frac{\left\| x - \bar{x}_i \right\|}{d} \tag{34}$$

where d is the actual support radius as shown in Fig. 18, which indicates the real region covered by the RBF. The results of the same MBB beam optimization are shown in Fig. 19. The value of d is taken as integer times an equivalent element size, which is calculated as

$$d = n \cdot \sqrt{m/e} \tag{35}$$

where n is a multiple of the element size, m is the area of the design domain, and e is the total number of elements. In this case, $m = 3$ and $e = 1000$. Figure 19 shows the results of $n = 2$, 4, 8, respectively. The actual size of the support area for each case is illustrated with a blue circle above each figure. The results suggest that the support radius is 2 to 4 times the equivalent element size and a very large support radius may cause instabilities during the optimization process. Compared with the MQ RBFs, the CS RBF provides a sparse matrix $\boldsymbol{A}$ in Eq. (13) and then, the computing efficiency is higher.

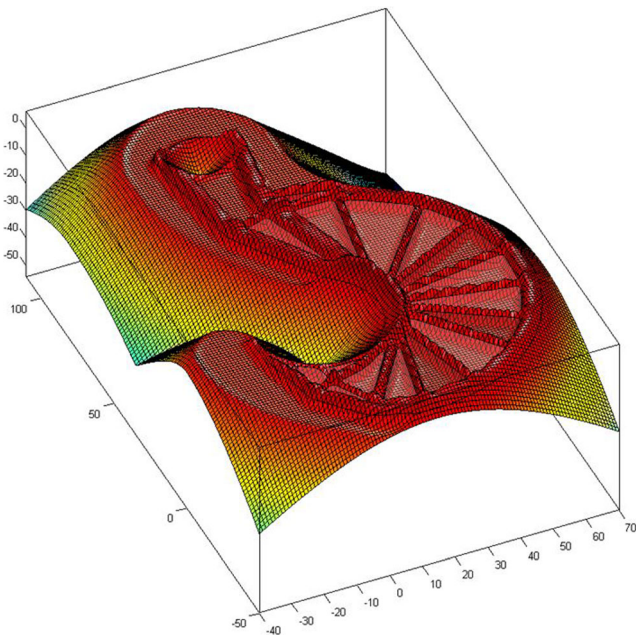

Fig. 21 The level set surface of the optimal results of the hook example

5.2 Examples of complex design domain problem

As mentioned before, the polygonal finite elements can be applied in solving irregular design domain, and the RBF-based level set method can be used in updating the front propagation in an unstructured grid. The combination of these two approaches can be easily implemented in solving the topology optimization problems in irregular design domains. Then, a hook example is implemented to illustrate the effectiveness of the proposed approach. The example is shown in Fig. 20 and the description of this example is defined in Fig. 7c of the literature (Talischi et al. 2012b). The problem definition is too complex to be described in detail, but the related original MATLAB file including the boundary conditions, geometry information, and loads can be downloaded in the Supplementary Material of Talischi et al. (2012b). The volume fraction is set to 0.4. Figure 20 a shows the definition of the problem in which the design is obviously irregular. Figure 20 b shows the optimal result obtained with the SIMP method with the code provided in (Talischi et al. 2012b) and Fig. 20c shows the optimal result obtained with the proposed method. Each of the two results is obtained with a mesh of 8000 elements. In the parameterized level set method, the multiquadratic spline is used with the parameter $c = 10^{-5}$. The mean compliance of result (b) is 7254.721, and the mean compliance of result (c) is 6907.560. The mean compliance of the proposed method is less than the result obtained with the SIMP method, but it is still hard to conclude which one is superior because the value of mean compliance is affected by a lot of parameters which may be totally different in the two models. However, the final topologies are quite similar.

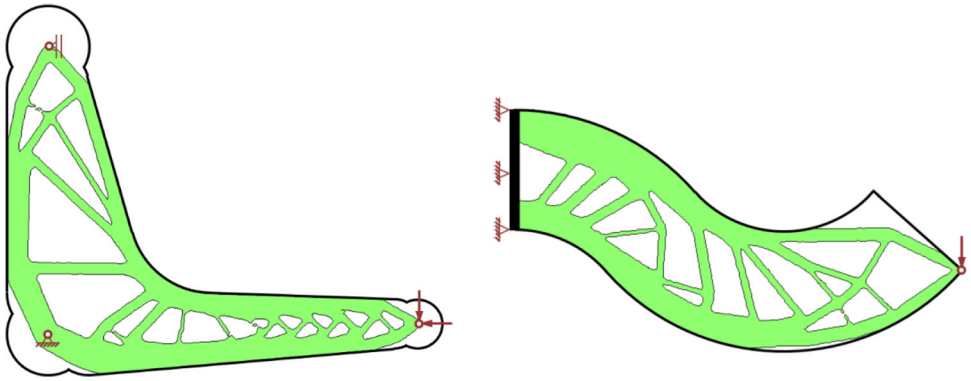

Fig. 22 The optimization results of two examples in (Talischi et al. 2012b) (**a** and **b**).

a The result of the wrench problem.

b The result of the curved cantilever beam.

The result with the SIMP method provides more details, which can be tuned with the radius of the filter and the proposed method provides smoother boundaries which are more suitable for manufacturing.

The level set surface of the result is shown in Fig. 21. Because the values of the level set function can only be accurately calculated inside the design domain, the values of the outside part shown in this figure are obtained by taking the minimum values of the interpolated values with RBFs and a signed distance function which is calculated in advance. The outside part is only calculated for display to illustrate the concept of the proposed method. It is not necessary to be calculated in each step because it has no effect on the result.

According to the figure, the value of the level set function shows a reasonable range in both the solid and void part of the design. Thus, the proposed approximative reinitialization combined with the implementation of the $\delta(\Phi)$ function can be considered to substitute for the conventional reinitialization approach, which is not very easy to implement in the parameterized level set model.

Two other examples in Talischi et al. (2012b) with polygonal finite elements are also studied as shown in Fig. 22, which further verifies the effectiveness of the proposed method.

6 Conclusions

In this paper, the parameterized level set method is combined with the polygonal finite element method to solve topology optimization problems on complex design domains, a problem that is difficult using traditional level set approaches. Two numerical schemes are applied with the proposed model. One is an approximate reinitialization scheme, which is proposed to substitute for the conventional reinitialization approach in conventional level set updating models; the other is the multiplication of a $\delta(\Phi)$ function to the velocity field to avoid numerical instabilities caused by infinite values of the level set function at some specific locations. The numerical examples demonstrate that the proposed parameterized level set method coupled with polygonal finite elements is robust. For example, an MBB beam was used to show that the designs obtained using the proposed scheme are not significantly dependent on the initial guess, the scheme allows for nucleation of holes, the method is not mesh sensitive as long as mesh quality is reasonable, and the method is not highly dependent on RBF parameters. Additionally, three problems on complex design domains are also presented. The parameterized level set method in this article does not implement any boundary smoothing scheme like perimeter control or filter, yet all result have smooth boundaries, which is always a favorable property of level set methods.

The parameterized level set method should also work well with other kinds of unstructured finite element meshes, like meshes with triangular elements or irregular quadrilateral elements. This has not been verified in this study, but schematically, there should be no difficulty because the updating of the parameterized level set function is in a parametric space instead of on a mesh grid. Another potential application of the parameterized level set method is in the geometric nonlinear optimization problems. Because the knots are not necessarily to be located in a fixed region, they can move around together with the deformed meshes. Thus, the numerical updating of the level set function can be handled easily as illustrated in this paper. Thus, the application of this method in problems of compliant mechanism design optimization should be straightforward.

Funding information This research was supported by the National Natural Science Foundation of China under Grant No. 11372004 and the State Scholarship Fund of China Scholarship Council under the Grant No. 201308440036.

Compliance with ethical standards

Conflict of interest The authors declare that they have no conflict of interest.

Replication of results As comprehensive implementation details are provided in the article, the results can be reproduced based on the published codes in the authors' previous papers which have been listed in the references. Scientists or interested parties are welcome to contact the authors for further explanations.

References

Allaire G, Jouve F, Toader A (2004) Structural optimization using sensitivity analysis and a level-set method. Journal of Computational Physics 194(1):363–393

Allaire G, Jouve F (2005) A level-set method for vibration and multiple loads structural optimization. Computer Methods in Applied Mechanics & Engineering 194:3269–3290

Barth TJ, Sethian JA (1998) Numerical schemes for the Hamilton-Jacobi and level set equations on triangulated domains. Journal of Computational Physics 145(1):1–40

Bendsoe MP, Kikuchi N (1988) Generating optimal topologies in structural design using a homogenization method. Computer Methods in Applied Mechanics and Engineering 71(2):197–224

Bendsoe MP (1989) Optimal shape design as a material distribution problem. Structural optimization 1(4):193–202

Cecil T, Qian J, Osher S (2004) Numerical methods for high dimensional Hamilton-Jacobi equations using radial basis functions. Journal of Computational Physics 196(1):327–347

Cheng KT, Olhoff N (1981) An investigation concerning optimal design of solid elastic plates. International Journal of Solids and Structures 17(3):305–323

Dapogny C, Faure A, Michailidis G, Allaire G, Couvelas A, Estevez R (2017) Geometric constraints for shape and topology optimization in architectural design. Computational Mechanics 59(6):933–965

Emmendoerfer H, Silva ECN, Fancello EA (2019) Stress-constrained level set topology optimization for design-dependent pressure load problems. Computer Methods in Applied Mechanics and Engineering 344:569–601

Gain AL, Paulino GH (2013) A critical comparative assessment of differential equation-driven methods for structural topology optimization. Structural and Multidisciplinary Optimization 48(4):685–710

Gelas A, Bernard O, Friboulet D, Prost R (2007) Compactly supported radial basis functions based collocation method for level-set evolution in image segmentation. IEEE Transactions on Image Processing 16(7):1873–1887

Guo X, Zhang W, Zhang J, Yuan J (2016) Explicit structural topology optimization based on moving morphable components (MMC) with curved skeletons. Computer Methods in Applied Mechanics & Engineering 310:711–748

Huang X, Xie YM (2010) Evolutionary topology optimization of continuum structures: methods and applications. John Wiley & Sons, Chichester

Isakari H, Kondo T, Takahashi T, Matsumoto T (2017) A level-set-based topology optimisation for acoustic–elastic coupled problems with a fast BEM–FEM solver. Computer Methods in Applied Mechanics and Engineering 315:501–521

Jiang L, Chen S, Jiao X (2018) Parametric shape and topology optimization: a new level set approach based on cardinal basis functions. International Journal for Numerical Methods in Engineering 114(1):66–87

Li H, Luo Z, Zhang N, Gao L, Brown T (2016) Integrated design of cellular composites using a level-set topology optimization method. Computer Methods in Applied Mechanics and Engineering 309:453–475

Liu J, Cheng L, To AC (2017) Arbitrary void feature control in level set topology optimization. Computer Methods in Applied Mechanics and Engineering 324:595–618

Liu Y, Li Z, Wei P, Wang W (2018) Parameterized level-set topology optimization method considering symmetry and pattern repetition constraints. Computer Methods in Applied Mechanics and Engineering 340:1079–1101

Luo Z, Tong L, Kang Z (2009) A level set method for structural shape and topology optimization using radial basis functions. Comput Struct 87(7-8):425–434

Luo Z, Tong L, Wang MY (2007) Shape and topology optimization of compliant mechanisms using a parameterization level set method. J Comput Phys 227(1):680–705

Luo Z, Wang MY, Wang SY, Wei P (2008) A level set-based parameterization method for structural shape and topology optimization. Int J Numer Methods Eng 76(1):1–26

Osher SJ, Santosa F (2001) Level set methods for optimization problems involving geometry and constraints: I. Frequencies of a two-density inhomogeneous drum. Journal of Computational Physics 171(1):272–288

Osher S, Sethian, JA (1988) Fronts propagating with curvature-dependent speed: Algorithms

Peng D, Merriman B, Osher S, Zhao H, Kang M (1999) A PDE-based fast local level set method. Journal of Computational Physics 155(2):410–438

Picelli R, Townsend S, Brampton C, Norato J, Kim HA (2018) Stress-based shape and topology optimization with the level set method. Computer Methods in Applied Mechanics and Engineering 329:1–23

Polajnar M, Kosel F (2017) Drazumeric R. Structural optimization using global stress-deviation objective function via the level-set method Structural and Multidisciplinary Optimization 55:91–104

Querin OM, Steven GP, Xie YM (1998) Evolutionary structural optimisation (ESO) using a bidirectional algorithm. Engineering Computations 15(8):1031–1048

Rozvany GIN, Zhou M, Birker T (1992) Generalized shape optimization without homogenization. Structural optimization 4(3-4):250–252

Sethian JA (1999) Level set methods and fast marching methods: evolving interfaces in computational geometry, fluid mechanics, computer vision, and materials science. Cambridge University Press

Sethian JA, Wiegmann A (2000) Structural boundary design via level set and immersed interface methods. Journal of Computational Physics 163(2):489–528

Sigmund O (2001) A 99 line topology optimization code written in Matlab. Structural and Multidisciplinary Optimization 21(2):120–127

Sigmund O, Maute K (2013) Topology optimization approaches: a comparative review. Structural and Multidisciplinary Optimization 48(6):1031–1055

Sukumar N, Tabarraei A (2004) Conforming polygonal finite elements. Int. J. Numer. Meth. Engng 61:2045–2066

Talischi C, Paulino GH, Pereira A, Menezes IFM (2010) Polygonal finite elements for topology optimization: a unifying paradigm. International Journal for Numerical Methods in Engineering 82(6):671–698

Talischi C, Paulino GH, Pereira A, Menezes IFM (2012a) PolyMesher: a general-purpose mesh generator for polygonal elements written in Matlab. Structural and Multidisciplinary Optimization 45(3):309–328

Talischi C, Paulino GH, Pereira A, Menezes IFM (2012b) PolyTop: a Matlab implementation of a general topology optimization framework using unstructured polygonal finite element meshes. Structural and Multidisciplinary Optimization 45(3):329–357

van Dijk NP, Maute K, Langelaar M, van Keulen F (2013) Level-set methods for structural topology optimization: a review. Structural and Multidisciplinary Optimization 48(3):437–472

Wang MY, Wang SY (2005) Parametric shape and topology optimization with radial basis functions. In: Proceedings of the IUTAM symposium on topological design optimization of structures, machines and materials: status and perspectives, Rungstedgaard, Denmark.

Wang MY, Wang XM, Guo DM (2003) A level set method for structural topology optimization. Computer Methods in Applied Mechanics and Engineering 192(1-2):227–246

Wang SY, Lim KM, Khoo BC, Wang MY (2007) An extended level set method for shape and topology optimization. Journal of Computational Physics 221(1):395–421

Wang SY, Wang MY (2006) Radial basis functions and level set method for structural topology optimization. International Journal for Numerical Methods in Engineering 65(12):2060–2090

Wang Y, Wang MY, Chen F (2016) Structure-material integrated design by level sets. Structural and Multidisciplinary Optimization 54(5): 1145–1156

Wei P, Li Z, Li X, Wang MY (2018) An 88-line MATLAB code for the parameterized level set method based topology optimization using radial basis functions. Structural and Multidisciplinary Optimization 58:831–849

Wei P, Wang MY (2006b) The augmented Lagrangian method in structural shape and topology optimization with RBF based level set method. The 4th China-Japan-Korea Joint Symposium on Optimization of Structural and Mechanical Systems, Kunming, China

Wei P, Wang MY (2006a) Parametric structural shape and topology optimization method with radial basis functions and level set method. Proceedings of IDETC/CIE 2006 ASME 2006 International Design Engineering Technical Conferences & Computers and Information in Engineering Conference, Philadelphia, USA

Wei P, Wang MY (2009) Piecewise constant level set method for structural topology optimization. Internat. J. Numer. Methods Engrg 78(4):379–402

Wendland H (1995) Piecewise polynomial, positive definite and compactly supported radial functions of minimal degree. Advances in Computational Mathematics 4:389–396

Xia L, Xia Q, Huang X, Xie YM (2018) Bi-directional evolutionary structural optimization on advanced structures and materials: a comprehensive review. Arch Computat Methods Eng 25(2):437–478

Xia Q, Shi T, Wang MY (2011) A level set based shape and topology optimization method for maximizing the simple or repeated first eigenvalue of structure vibration. Structural and Multidisciplinary Optimization 43(4):473–485

Xie X, Mirmehdi M (2011) Radial basis function based level set interpolation and evolution for deformable modelling. Image and Vision Computing 29(2-3):167–177

Xie YM, Steven GP (1993) A simple evolutionary procedure for structural optimization. Computers & Structures 49(5):885–896

Yamada T, Izui K, Nishiwaki S, Takezawa A (2010) A topology optimization method based on the level set method incorporating a fictitious interface energy. Computer Methods in Applied Mechanics and Engineering 199(45-48):2876–2891

Zhang WS, Guo X, Wang MY, Wei P (2013) Optimal topology design of continuum structures with stress concentration alleviation via level set method. International Journal for Numerical Methods in Engineering 93(9):942–959

Zhou Y, Zhang W, Zhu J, Xu Z (2016) Feature-driven topology optimization method with signed distance function. Computer Methods in Applied Mechanics & Engineering 310:1–32